

Effect of High Strain Rate on Tensile Strength of SHCCs in Comparison to that of FRHSCs

*Shasha Wang¹⁾ and Hoang Thanh Nam Le²⁾

¹⁾ Engineering Institute of Technology, Victoria, Australia

²⁾ Sika Limited (Vietnam), Dong Nai, Vietnam

¹⁾ shasha.wang@eit.edu.au

ABSTRACT

This paper presents an experimental study on the effect of high strain rate on the tensile behavior of two Strain-Hardening Cement Composites (SHCCs), compared to that of Fiber-Reinforced High-Strength Concretes (FRHSCs) with similar compressive strength. One of the SHCCs was reinforced with 2% of polyvinyl alcohol (PVA) fibers by volume (SHCC-PVA) and had a compressive strength of 62 MPa. The other was reinforced with 0.5% of steel plus 1.5% of polyethylene (PE) fibers by volume (SHCC-ST+PE) and had a compressive strength of 80 MPa. The two FRHSCs were reinforced with 0.5% of steel fibers, and had compressive strengths of 61 MPa and 85 MPa, respectively.

A split Hopkinson pressure bar facility was used to determine the splitting tensile behavior of the SHCCs and FRHSCs at strain rates from about 1 to 11 s⁻¹. The Dynamic Increase Factor ($DIF_{\bar{t}}$), the ratio of the splitting tensile strength under dynamic loading to that under static loading, was determined for the materials considered. A high-speed camera was also used to capture the failure process of the dynamic splitting tensile tests. The results indicate that the $DIF_{\bar{t}}$ of the SHCCs was lower than that of the FRHSCs at a similar strain rate. In addition, it is shown that the equations in CEB-FIP 1990 and fib 2010 codes are not applicable to SHCCs and FRHSCs at the strain rates from about 1 to 11 s⁻¹. The transition strain rates of these SHCCs and FRHSCs seem to be lower than the values of 30 and 10 s⁻¹ recommended by the CEB-FIP 1990 and fib 2010 codes, respectively.

1. INTRODUCTION

In recent decades, behavior of concrete materials and structures under high strain rate loading conditions such as impact and blast has gained increased attention among researchers and relevant stakeholders. Effect of high strain rate on the compressive

¹⁾ Lecturer

²⁾ Technical Service Manager

behavior of plain and fiber-reinforced concrete, normal strength and high strength concrete and even ultra-high performance cementitious composites such as strain-hardening cement composites (SHCC), or sometimes referred to as engineered cementitious composites (ECC) have been extensively investigated and reported in literature. Studies on the tensile behavior of these materials, however, are still relatively limited, which could be partially attributed to the fact that there is a lack of standard test methods to determine tensile properties of concrete-like materials at high strain rate loading conditions. Failure mechanism of localized damage to high-velocity projectile impact, a typical scenario of materials and structures in high-strain rate loading conditions, indicates presence of tensile waves and damage resulting from tensile stress exceeding dynamic tensile strength. It is thus interesting to investigate the effect of high strain rate on the tensile behavior of these materials in order to understand their performance for optimum design of protective structures against severe loading conditions.

2. EXPERIMENTAL DETAILS

2.1 Mixtures

Mix Proportions Two Strain-Hardening Cement Composites (SHCCs) and two Fiber-Reinforced High-Strength Concretes (FRHSCs) were investigated in this study and the mix proportions of them are given in Table 1.

The SHCC-PVA was a revised mixture based on a SHCC mixture from literature (Wang 2011). The SHCC-ST+PE was a mixture developed by another research group at National University of Singapore (Maalej 2005). The two SHCCs had the same w/cm (water to cementitious materials ratio) and total volume of fibers. The SHCC-PVA was reinforced with 2% polyvinyl alcohol (PVA) fibers, whereas the SHCC-ST+PE contained 0.5% steel fibers (ST) and 1.5% polyethylene (PE) fibers.

The two FRHSCs were designed to have similar compressive strengths with that of the SHCCs, respectively. Both of them were reinforced with 0.5% of steel fibers by volume of the mixtures.

Table 1. Mix proportions (kg/m³) of mixtures

Mixture	w/cm	C	MA	water	CA	Sand	Fiber	VMA	SP
FRHSC-60	0.50	410	-	205	946	760	39	-	3
FRHSC-85	0.35	500	-	175	900	744	39	-	8
SHCC-PVA	0.25	587	704 (FA)	323	-	469 [#]	26	2.9	10*
SHCC-ST+PE	0.25	1478	148 (SF)	414	-	-	39+14.4 ST+PE	-	17

w/cm: water to binder ratio; C: Cement; MA: Mineral Admixture; CA: Coarse Aggregate; VMA: Viscosity Modifying Admixture; SP: superplasticizer; FA: Fly Ash; SF: Silica Fume; ST: Steel fiber; PE: Polyethylene fiber; * polycarboxylate-based superplasticizer; [#] sieved quartz sand with a maximum size of 0.25 mm

Materials The steel fibers used in the two FRHSCs and the SHCC-ST+PE had a length of 13 mm and a length to diameter ratio of 81. Both the PVA in the SHCC-PVA

and the PE fibers in the SHCC-ST+PE had a length of 12 mm, and their length to diameter ratios were 300 and 308, respectively. The Young's moduli of the steel, PVA and PE fibers were 200, 41, and 66 GPa, respectively. The tensile strengths of them were 2500, 1612, and 2610 MPa, respectively.

In addition to ASTM Type I normal Portland cement in all the mixtures, fly ash and silica fume were also used in the two SHCCs, respectively, as supplementary cementitious materials. Crushed granite coarse aggregate with a nominal maximum size of 12.5 mm and specific gravity of 2.65 and natural sand with a specific gravity of 2.63 were used in the FRHSCs. Sieved sand with a maximum size of 0.25 mm was used in the SHCC-PVA, and no sand was used in the SHCC-ST+PE. Viscosity modifying admixture (VMA) was used in the SHCC-PVA to disperse the fibers properly and to prevent bleeding of the fresh mixture. A polycarboxylate-based superplasticizer (SP) was used in the SHCC-PVA, whereas a naphthalene-based superplasticizer was used in all the rest mixtures to increase their workability.

Workability The FRHSCs were mixed in a large pan mixer, whereas the SHCCs were mixed in a Hobart mixer. The fibers were added last. Immediately after mixing, the workability of the fresh mixture was determined. Vebe time for FRHSC-60 and FRHSC-85 was 8 and 9 sec, respectively. Flow table value for SHCC-PVA and SHCC-ST+PE was 165 and 150 mm, respectively.

2.2 Specimens

For each mixture, three 100 mm cubes and three 100×100×400-mm prisms were prepared for 28-day compressive strength and flexural tensile strength tests. Three standard cylinders (Φ 100×200-mm) were also prepared for each mixture to determine the compressive strength, Young's modulus, and Poisson's ratio at 28 days. Short cylindrical specimens (Φ 77×39-mm) were prepared for the determination of splitting tensile strength in both static and dynamic conditions. The Φ 77 mm cylinders were cast in PVC molds with a height of about 200 mm. They were then cut and ground into the desired thickness of about 39 mm during the 15th to 21st days. The molded specimens were covered with wet linen and plastic sheets for the first 24 hrs and were then transferred to a fog room and cured for another 20 days at temperatures around 28 - 30°C. After that, the specimens were placed in a chamber with a controlled temperature of 30°C and a relative humidity of 65% until the testing date.

The static and dynamic splitting tensile tests were conducted at the age of at least 2 years (2-6 years), whereas other static properties were determined at the age of 28 days. The specimens for the static and dynamic splitting tensile tests were kept in the controlled humidity and temperature environment for at least two years to ensure a consistent moisture condition, since the moisture condition of the cement-based materials has a significant influence on its properties under high strain-rate loadings.

2.3 Test Methods

Static Properties A servo-hydraulic material test system (MTS) was used to determine the compressive strength (100-mm cubes and Φ 100×200-mm cylinders). It was also used to test the Young's moduli, and Poisson's ratios following ASTM C469 (Φ 100×200-mm cylinders) with strain gauges mounted at the mid-height of the specimens. A

hydraulic Instron machine was employed to determine the flexural behavior of the 100×100×400-mm specimens following the ASTM C1609 guideline.

The static splitting tensile strength was determined by a Control's Automax 5 compression tester based on the $\Phi 77 \times 39$ -mm cylinders. Thin plywood bearing strips satisfying ASTM C496/C496M were placed between the specimen and both the upper and lower bearing blocks of the testing machine.

The loading rate was about 10^{-5} s^{-1} for these static tests.

Dynamic Splitting Tensile Strength Split Hopkinson pressure bar (SHPB) has been used by researchers to measure the dynamic splitting tensile strength of concrete-like materials (Chen 2014; Zhao 2020). In this study, an SHPB with both the input and output bars having a diameter of 80 mm and a length of 5 m as shown in Fig. 1 was used to determine the dynamic splitting tensile strengths of the mixtures at strain rates ranging from about 1 to 11 s^{-1} . Cylindrical specimens with the sizes of $\Phi 77 \times 39$ -mm were selected for the test specimens, considering the molds available and the maximum aggregate size. They were of the same size as those used for static splitting tensile tests aiming to minimize the possible effect from size.

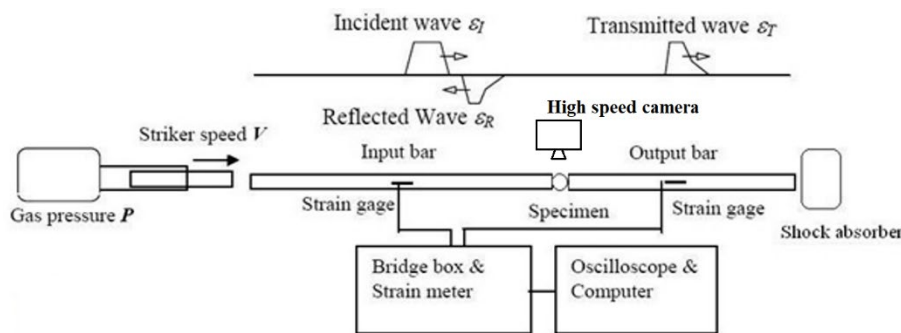


Fig. 1. Schematic setup of splitting tensile test using SHPB (modified from User's Manual provided by SHPB equipment supplier)

The equipment consisted of a launching system, striker, input bar, output bar, shock absorber, and a data acquisition system. During the test, the striker was launched by compressed gas towards the input bar, which generated an incident compressive wave propagating through the bars and the specimen. The wave was partially reflected from and partially transmitted into the specimen at the input bar and specimen interface. The transmitted wave traveled into the specimen and would experience reflection and transmission at the interface of the specimen and output bar. Two strain gauges were attached at the mid-point of the input bar to measure the time dependent incident wave for incident strain history ϵ_i and reflected wave for reflected strain history ϵ_r , and another two at the mid-point of the output bar to measure the transmitted wave for transmitted strain history ϵ_t . Signals from the strain gauges were captured by an oscilloscope at $0.5 \mu\text{s}$ intervals, corresponding to a sampling rate of 2,000,000 data points per second. In

addition, a high-speed camera was used to capture the failure process of the specimens at a rate of 50,000 frames per second.

A 1-mm thick aluminum disc with a diameter ranging from 25 to 28.5 mm was pasted on the center of impact surface of the input bar as the pulse shaper by a thin layer of grease in the SHPB tests to prolong the rising time and to filter out the high frequency components of the incident waves.

Since the stress distribution in the specimen at failure is similar for both the dynamic and static tests (Tedesco 1990) according to the stress distribution in a specimen during the static splitting tensile test, the following equation used to calculate static splitting tensile strength can also be used to calculate the dynamic tensile strength ($f_{t,d}$) determined using SHPB.

$$f_{t,d} = \frac{2P}{\pi LD} \quad (1)$$

where P is the peak load applied on the specimen. which can be calculated by $P = \pi R_b^2 \sigma_{t,max} = \pi R_b^2 E_b \varepsilon_{t,max}$, with R_b , $\sigma_{t,max}$, E_b and $\varepsilon_{t,max}$ being the radius of the SHPB bars, the peak transmitted stress in the output bar, Young's modulus of the SHPB bars, and the peak transmitted strain in the output bar, respectively. L is the specimen length, and D is the specimen diameter.

The strain rate is evaluated by the average strain rate ($\dot{\varepsilon}$) of the specimen tested based on the transmitted strain (ε_t). It can be determined by the following equation:

$$\dot{\varepsilon} = \frac{\dot{\sigma}}{E} = \frac{1}{E} \frac{f_{t,d}}{\tau} \quad (2)$$

where $\dot{\sigma}$ is the average stress rate in the specimen, and E is the Young's modulus of the specimen; τ is the time lag between the start of the transmitted stress wave pulse and the maximum transmitted stress.

In general, splitting tensile test results are valid if the crack is initiated at the center of the specimen and propagates in the direction of the diameter where the load is applied. If cracks other than this, e.g. crushing at the loading points happens first, the experiment is invalid. Hence, it is important to check the validity of the experiment before processing the results.

Fig. 2 shows the failure process of an FRHSC-60 specimen captured by the high-speed camera during the dynamic splitting tensile test with a time interval of 20 μ s. The red circle highlights the first appearance of cracks captured by the camera, which occurred at 40 μ s from the impact on the specimen. Apparently, initial cracks occurred at the center of the specimens, and also the cracks developed along the loading diameter direction before linking the two loading points. Similar phenomenon was observed for other specimens and other mixtures as well. These are the evidence for the validity of current experiments. Some specimens after the tests exhibited triangular crush zones at the two impact points. However, such localized crush occurred after the initial cracks at the center of the specimen and the time reaching the peak load which was typically around 100-150 μ s as recorded by the high-speed camera synchronized with the data acquisition system (oscilloscope).

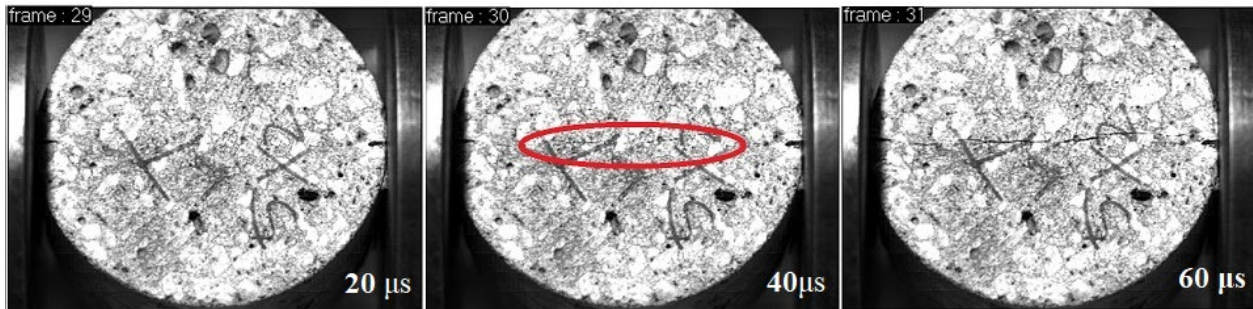


Fig. 2. Failure process of an FRHSC-60 specimen captured by high-speed camera during SHPB splitting tensile tests

3. RESULTS AND DISCUSSION

3.1 Static Properties

Compressive Strength, Young's Modulus and Poisson's Ratio. Typical static properties of the FRHSCs and SHCCs are summarized in Table 2.

The strength values based on the 100 mm cubes are generally slightly higher than the corresponding values based on the $\Phi 100 \times 200$ mm cylinders for the materials, which can largely be attributed to the smaller aspect ratio and hence more influence from end friction of the cubes than the cylinders. Referring to the values based on the cylinders, similar compressive strength was achieved for the FRHSC-60 and the SHCC-PVA and for the FRHSC-85 and the SHCC-ST+PE-85, respectively.

The SHCCs have significantly lower densities and Young's moduli than the FRHSCs due to the absence of coarse aggregate in the former. The Poisson's ratios of the two SHCCs (0.23-0.26) are slightly higher than those of the FRHSCs (0.20-0.21), probably at least partly attributing to the absence of coarse aggregate in the SHCCs.

Table 2. Static properties of the materials

Mixture	Density kg/m ³	compressive strength		Young's modulus GPa	Poisson's ratio	splitting tensile strength MPa	flexural strength MPa
		cube MPa	cylinder MPa				
FRHSC-60	2424	75.9	60.5	38.1	0.21	7.1	7.1
FRHSC-85	2418	94.2	85.4	37.7	0.20	9.1	7.2
SHCC-PVA	2033	66.9	62.0	23.4	0.23	9.1	10.7
SHCC-ST+PE	2111	83.9	80.4	21.1	0.26	9.8	11.1

Tensile Behavior. The splitting tensile strengths and flexural strengths of the four mixtures are summarized in Table 2 as well. Generally speaking, the splitting tensile strength of a concrete is slightly lower than the flexural tensile strength (Mindess 2003).

In this study, the splitting tensile strength of the mixtures is not consistently lower than the corresponding flexural tensile strength probably due to the much smaller size ($\Phi 77 \times 39$ -mm vs. $100 \times 100 \times 400$ -mm), much older testing age (2-6 years vs. 28 days), and drier condition (placed in constant humidity room for 2-6 years vs. 7 days until tests) of the specimens used for the splitting tensile tests than for the flexural tensile tests, as well as the presence of fiber reinforcement in the specimens.

The flexural load versus deflection behavior of the four types of the materials is depicted in Fig. 3. Different from the FRHSCs, the SHCCs exhibited strain hardening behavior as seen from their increased load carrying capacities after the first peak until the ultimate peak and hence have much larger areas under the post peak load versus deflection curves. Before reaching the ultimate value, the load carrying capacity of the SHCCs experienced some drops and rises. Each drop indicates localization of a new crack, while each rise indicates the crack arresting by intercepting fibers which results in stress redistribution and generation of new crack at a different location. These lead to the multiple cracking properties of the SHCCs in the flexural test. In addition, at a given deflection in the post peak portion of the curves, the load carrying capacity of the SHCC-ST+PE is higher than that of the SHCC-PVA. Similarly, the post peak load carrying capacity of the FRHSC-85 is higher than that of the FRHSC-60. These may be attributed to the higher matrix strength and better bond between the matrix and fibers arising from the reduced w/cm in the SHCC-ST+PE and FRHSC-85 than in the SHCC-PVA and FRHSC-60, respectively. For the SHCC-ST+PE, the better bonding also benefits from the extremely fine silica fume particles.

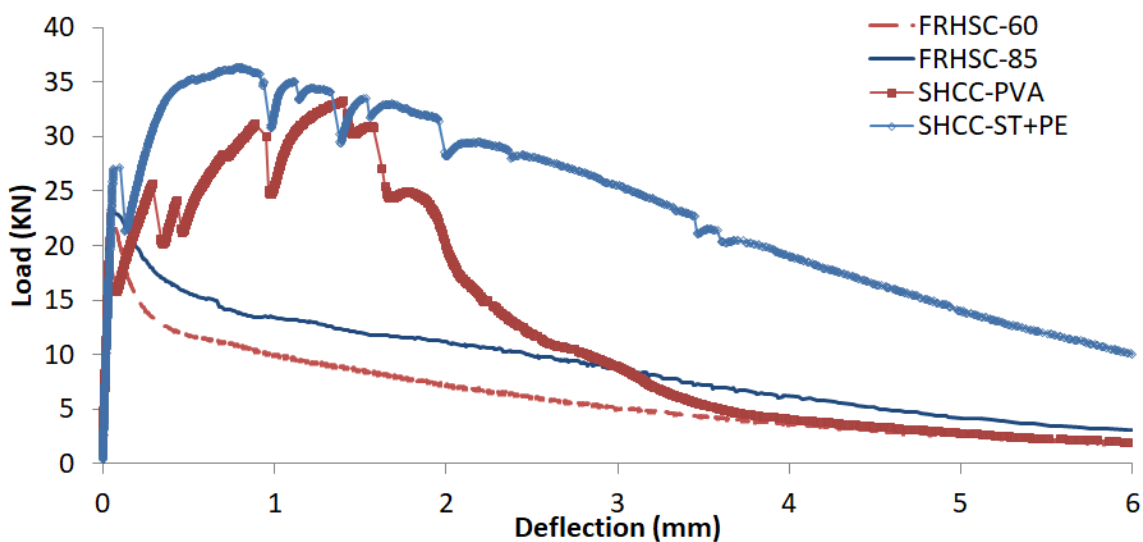


Fig. 3. Flexural tensile behavior of mixture determined on $100 \times 100 \times 400$ -mm beams.

3.2 Splitting Tensile Behavior determined by SHPB

Dynamic Splitting Tensile Strength and Dynamic Increasing Factor The dynamic increase factor (DIF_{ft}), the ratio of the splitting tensile strength under dynamic loading

determined by SHPB to that under static loading, was determined and depicted in Fig. 4. The recommended values based on the CEB-FIP 1990 (1993) and fib 2010 (2013) equations as well as those from the well-recognized modified equation by Malvar and Ross (1998) are also plotted in Fig. 4 as benchmarks.

It can be seen from the figure that the DIF_{ft} for all the four mixtures increases with an increase in the strain rate within the experimental range of $1-11 \text{ s}^{-1}$. Such increasing trend of splitting tensile strength with strain rate is consistent with that reported in literature for dynamic strength of most cement-based materials at similar strain rate ranges.

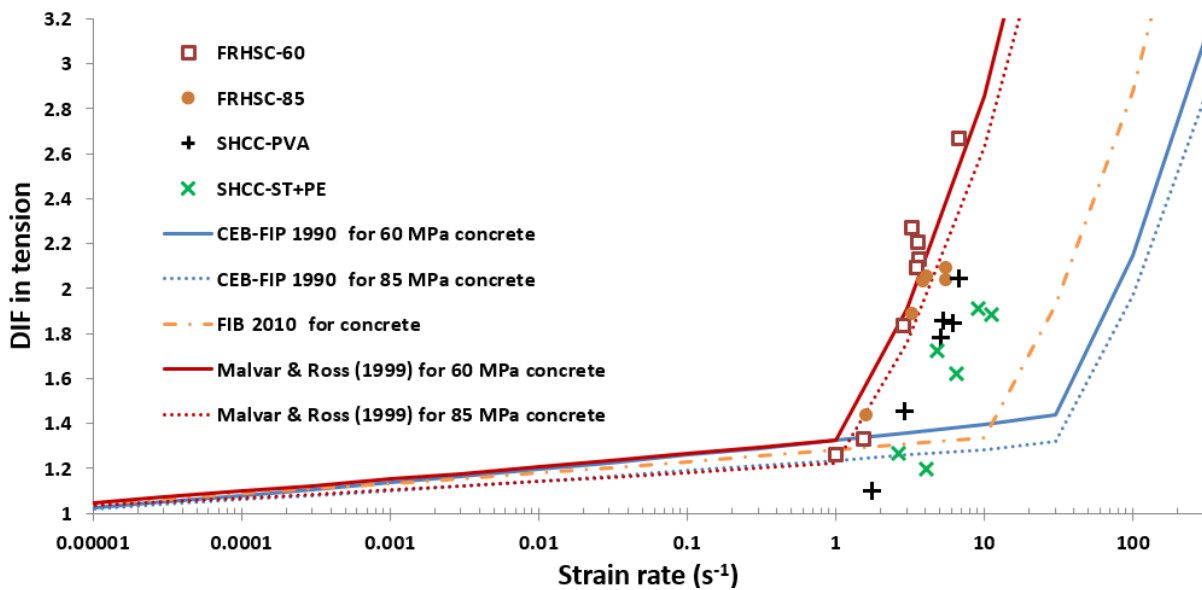


Fig. 4. DIF of splitting tension strength determined in comparison with DIF in tension values recommended by codes and other recommendations.

In addition, both the CEB-FIP and fib equations significantly underestimate the DIF_{ft} values for both the FRHSCs and SHCCs. The DIF_{ft} values based on the modified equation by Malvar and Ross (1998) are closer to the experimental results determined in this study, especially for the two FRHSCs. The values of the transition strain rate $\dot{\epsilon}_t$, beyond which there is a sharp increase in slope of the DIF curve, of the SHCCs and FRHSCs seem to be lower than the values of 30 and 10 s^{-1} recommended by the CEB-FIP 1990 and fib 2010 code for plain concrete, respectively. The $\dot{\epsilon}_t$ of the FRHSCs seems to be around 1 s^{-1} as recommend by Malvar and Ross (1998), whereas those of the SHCCs appear to be slightly higher and may fall between 1 and 3 s^{-1} as predicted from Fig. 4. The relatively higher $\dot{\epsilon}_t$ of the SHCCs than the FRHSCs may be attributed to the higher fiber contents in the former. Dispersed fibers can hold the hardened matrices together and reduce the lateral expansion of the specimens. Hence, a higher $\dot{\epsilon}_t$ may be required to trigger the change of the behavior for mixtures reinforced by more fibers.

SHCC vs. FRHSC in Dynamic Splitting Tensile Behavior As indicated in Fig. 4, the DIF_{ft} values of the SHCCs are lower than those of the FRHSCs of corresponding strength at a similar strain rate. The trend is consistent with the findings on DIF in compression in a previous study (Wang 2017). As discussed extensively in that paper, SHCC is less sensitive to high strain rate than FRHSC of a similar strength. The lower strain rate sensitivity of the SHCCs can be attributed to the higher fiber content and absence of coarse aggregates.

Also, the SHCC and the FRHSC specimens had slightly different failure patterns. Fig. 5 compares the images of specimens from each mixture captured by the high-speed camera at 100 μ s from the impact on the specimens. As can be observed, for the FRHSC specimens, there was typically only one main crack running through the loading direction, which then separated the specimen into two halves. However, for the SHCC specimens, there were a couple of approximately parallel cracks in the loading direction, and the specimens were still in one piece after the tests. This multiple cracking phenomenon of the SHCC specimens under dynamic splitting tensile tests is similar to what was observed in static loading conditions, which can be attributed to the specific mix design of the SHCC mixtures. The damage degree of the SHCC specimens after the tests also benefits from the mix design and especially the high fiber volume content of the SHCC.

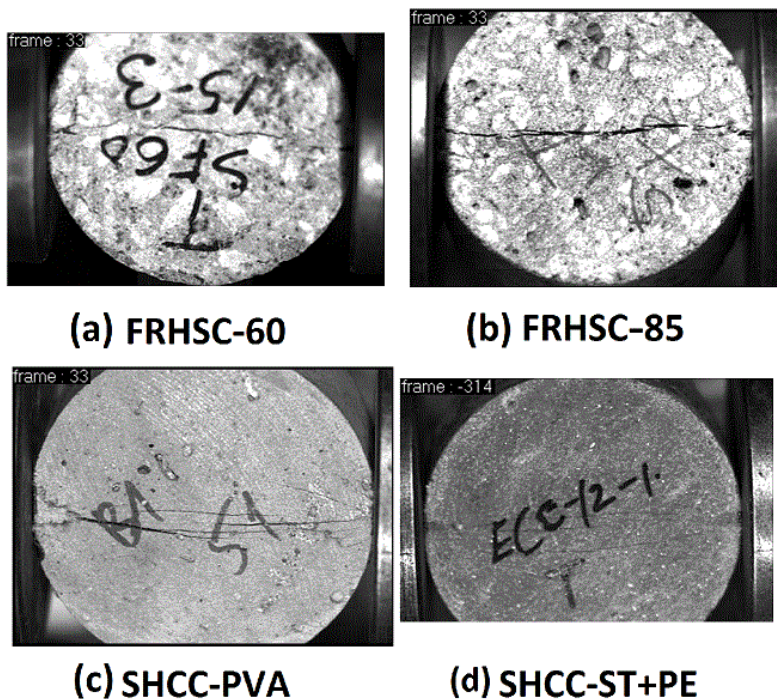


Fig. 5. Images captured by high-speed camera at 100 μ s from impact on specimen during SHPB splitting tensile tests.

Effect of Compressive Strength on DIF_{ft} Fig. 4 above also indicates that the DIF_{ft} values of the SHCC-ST+PE are generally lower than those of the SHCC-PVA at a similar strain rate in the range tested, and the DIF_{ft} values of the FRHSC-85 appear to be slightly

lower than those of FRHSC-60. This indicates that the strain rate sensitivity of SHCCs and FRHSCs in tension is affected by their static compressive strengths. This is also consistent with the findings for strain rate sensitivities of these materials in compression in a previous study (Wang 2017). In brief, strength enhancement of concrete-like materials at high strain rates can be partially attributed to the fact that cracks do not have enough time to go around the aggregates through the interfacial transition zone (ITZ), which is typically the weakest link within the composites, but have to go through the aggregates, which is generally stronger. For a concrete of a higher strength, ITZ is improved and may no longer be the weakest link. The strength enhancement due to change of crack paths becomes less significant because the improved ITZ has already contributed to the static strength of the mixture. More detailed discussion of the mechanism behind the lower strain rate sensitivity of the material with a higher static compressive strength can be found in the previous work (Wang 2017).

4. CONCLUSIONS

The effect of strain rate on the tensile behavior of two Strain-Hardening Cement-Composites (SHCCs) was investigated and compared against those of two Fiber-Reinforced High-Strength Concretes (FRHSCs) of similar compressive strengths. The dynamic splitting tensile strength or the DIF_t of the SHCCs and FRHSCs increases with strain rate. The strain rate sensitivity of the SHCCs is lower than that of the FRHSCs in the strain rate range tested. Within the two SHCCs and the two FRHSCs, the strain rate sensitivity appears to be lower for the mixture with a higher static compressive strength, albeit not significantly as indicated by the relatively limited experiment data in this study. Also, CEB-FIP 1990 and fib 2010 codes equations underestimate the DIF_t of the SHCCs and FRHSCs at the strain rates from about 1 to 11 s⁻¹ and appear to overestimate the transition strain rates.

ACKNOWLEDGEMENT

The experimental work in this paper was conducted when the authors were at National University of Singapore (NUS). The work in this paper was done under the supervision of Professor Min-Hong Zhang, who is now retired from NUS.

REFERENCES

- Chen, J. J., Guo, B. Q., Liu, H. B., Liu, H., and Chen, P. W. (2014), "Dynamic Brazilian Test of Brittle Materials Using the Split Hopkinson Pressure Bar and Digital Image Correlation." *Strain*, **50**(6), 563–570.
- COMITE EURO-INTERNATIONAL DU BETON, (1993). CEB-FIP Model Code 90, Thomas Telford.

- Maalej, M., Quek, S. T., and Zhang, J. (2005), "Behavior of Hybrid-Fiber Engineered Cementitious Composites Subjected to Dynamic Tensile Loading and Projectile Impact.", *J. Mater. Civil Eng.*, **17**(2), 143–152.
- Malvar, L. J., and Ross, C. A. (1998), "Review of Strain Rate Effects for Concrete in Tension." *ACI Mater. J.*, **95**(6).
- Mindess, S., Young, J. F., and Darwin, D. (2003), *Concrete* (2nd ed.), Prentice Hall.
- Tedesco, J. W. (1990), *Numerical Analysis of Dynamic Splitting-Tensile and Direct Tension Tests*, Air Force Engineering and Service Center.
- Walraven, J., and Vliet, A. B. (2013), *fib Model Code for Concrete Structures 2010*, Ernst & Sohn Publishing House.
- Wang, S., Le, H. T. N., Poh, L. H., Quek, S. T., and Zhang, M.-H, (2017), "Effect of high strain rate on compressive behavior of strain-hardening cement composite in comparison to that of ordinary fiber-reinforced concrete." *Constr. Build. Mater.*, **136**, 31–43.
- Wang, S. and Li, V. (2006), "Polyvinyl Alcohol Fiber Reinforced Engineered Cementitious Composites: Material Design and Performances", *Proceedings of International RILEM Workshop on HPFRCC in Structural Applications*, Hawai'i.
- Zhao, X., Li, Q., and Xu, S. (2020), "Contribution of steel fiber on the dynamic tensile properties of hybrid fiber ultra high toughness cementitious composites using Brazilian test." *Constr. Build. Mater.*, **246**, 118416.